ACS OMEGA

http://pubs.acs.org/journal/acsodf

Article

Screening Multidrug Resistance Reversal Agents in Traditional Chinese Medicines by Efflux Kinetics of D-Luciferin in MCF-7/DOX^{Fluc} Cells

Yue Zhao,[#] Chaoyuan Tang,[#] Jingyi Huang,[#] Hongyan Zhang, Jingbin Shi, Shujun Xu, Lisha Ma, Chun Peng, Qi Liu, and Yang Xiong*

Cite This: *ACS Omega* 2023, 8, 4853−4861

Read Online

ACCESS | Metrics & More | Article Recommendations | Supporting Information

ABSTRACT: In this study, we established a simple and rapid *in vitro* method for screening multidrug resistance (MDR) reversal agents in traditional Chinese medicines (TCMs), which could better correspond to the MDR reversing effect *in vivo*. Here, D-luciferin, a substrate for the enzyme firefly luciferase and also a substrate for ATP-binding cassette transporters (ABC transporters), was used as the probe to detect its efflux kinetics caused by ABC transporters. First, we established a stable doxorubicin (DOX)-resistant cell line (MCF-7/DOX^{Fluc}) that overexpressed luciferase. Then, some kinds of TCMs were chosen for the MDR reversal agents to measure its effect on inhibiting the D-luciferin outflow from MCF-7/DOX^{Fluc}, and the ideal reversal agent with the least D-luciferin efflux from MCF-7/DOX^{Fluc} was selected to further investigate its effect combined with DOX on MCF-7/DOX^{Fluc} tumor-bearing mice. The results indicated that quercetin (Qu) could remarkably increase the retention of D-luciferin in MCF-7/DOX^{Fluc} *in vitro* and *in vivo*. Also, the combination of Qu and DOX could exceedingly inhibit the tumor growth, which proved the feasibility of this *in vitro* screening method. The study proposed a feasible method for mass screening of MDR agents from TCMs *in vitro*.

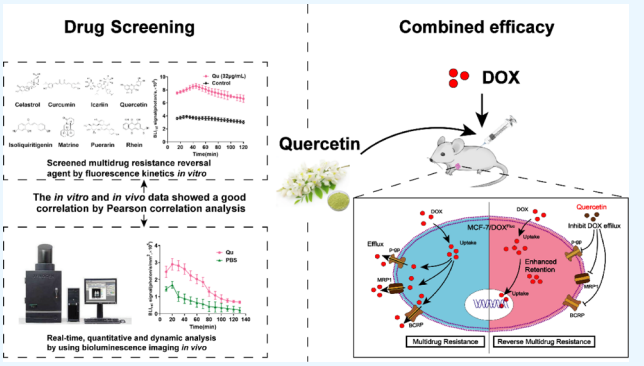

INTRODUCTION

Breast cancer is the main cause of mortality for female cancer patients worldwide, and drug resistance is still the key factor.[1,2] Chemotherapy is still the main therapeutic modality for cancer treatment.[3] However, multidrug resistance (MDR) is the major cause of chemotherapy failure in breast cancer.[4] Therefore, it is important to find an effective and safe MDR reversal agent.

At present, MDR reversal agents mainly include chemical agents represented by verapamil (Vera).[5] Besides chemical agents, many traditional Chinese medicines (TCMs) can be used as MDR reversal agents, and some of them even have certain anti-tumor effects.[6,7] Moreover, TCMs have multi-component and multi-target characteristics, which can effectively reverse the MDR resulting from multiple mechanisms.[8,9] However, with the complexity and diversity of TCM components, it is important to establish a method for *in vitro* rapid batch screening of MDR reversal agents that should be safe and effective *in vivo*.

As numerous studies demonstrated, the function of the family of ATP-binding cassette transporters (ABC transporters) is one of the causes of MDR.[10,11] The emergence of MDR mediated by ABC transporters, containing multidrug resistance protein 1 (MRP1), breast cancer resistance protein (BCRP), and *P*-glycoprotein (*P*-gp), often hinders cancer treatment.[12,13] It is now believed that the effect of MDR reversal agents is mostly related to the efflux function of ABC transporters.[14] The ABC transporters actively transport chemotherapeutic drugs out of cells, thereby reducing their cytotoxic effects.[15,16] Thus, inhibiting the chemotherapeutic drugs efflux from cancer cells will be an important strategy to overcome MDR.

There have been many *in vitro* probes to screen the MDR reversal agents. For example, rhodamine worked as a probe to detect the efflux function of ABC transporters.[17,18] However, these methods cannot enable the real-time imaging of efflux kinetics of MDR protein substrates directly *in vivo*. In addition, the tumor microenvironment is different *in vitro* and *in vivo* remarkably,[19] and thus, it is difficult to quickly determine the consistency of efflux kinetics *in vitro* and *in vivo* after treating with MDR reversal agents. Here, we established a method to monitor in real time the efflux kinetics of the MDR protein

Received: November 3, 2022
Accepted: January 5, 2023
Published: January 23, 2023

substrates affected by MDR reversal agents *in vitro*, which could keep the high consistency in evaluating the *in vivo* effect of MDR reversal agents.

Since many chemotherapeutic drugs are the substrates of ABC transporters,[20] we chose D-luciferin, which is also a substrate of ABC transporters,[21,22] to evaluate the efflux function of MDR proteins before and after the TCM treatment. Here, we established a stable doxorubicin (DOX)-resistant cell line (MCF-7/DOX^{Fluc}) with overexpressed luciferase. Since only the D-luciferin entering tumor cells can emit light, this method can measure the efflux function of MDR proteins in MCF-7/DOX^{Fluc} cells *in vitro* and *in vivo* (Figure 1). The efflux kinetics of

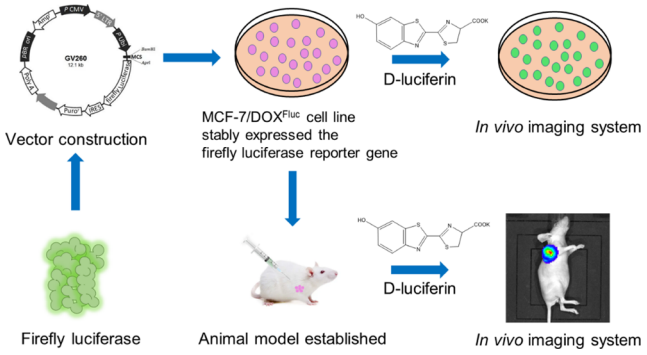

Figure 1. Outline of the experimental design and flow of the D-luciferin and MCF-7/DOX^{Fluc} assay system.

D-luciferin after the treatment with MDR reversal agents in TCMs were recorded by bioluminescence imaging (BLI), and the *in vitro*−*in vivo* correlation coefficient was calculated by Pearson correlation analysis. Next, the *in vivo* anti-tumor efficacy of the ideal reversal agent combined with DOX in MCF-7/DOX^{Fluc} bearing mice was investigated, and the content of DOX in the tumor was measured by high-performance liquid chromatography (HPLC). These two methods both could further testify the effect of this MDR reversal agent.

RESULTS

Screening MDR Reversal Agents in TCMs by Efflux Kinetics of D-Luciferin from MCF-7/DOX^{Fluc}. It could be found that the photons of the bioluminescence signal were linearly related to the content of D-luciferin, below the fluorescein substrate saturation threshold, and also linearly related to the tumor cell number (Figure S1). Next, the IC_{50} value of MCF-7/DOX^{Fluc} after the treatment by a series of TCM components were measured using a 3-(4, 5-dimethylthiazol-2-yl)-2,5-diphenyltetrazolium bromide (MTT) assay (Figure 2A). After that, the bioluminescence signal was used to draw the efflux curve of D-luciferin for each group (Figures 2B and S2), and the non-compartment model was used to calculate the efflux kinetics parameters. The results showed that compared to 0.1% dimethyl sulfoxide (DMSO), curcumin (Cur), quercetin (Qu), coixenolide (Coix), icariin (Ica), rhein (Rh), celastrol (Cel), and isoliquiritigenin (Iso) increased the area under the curve (AUC) of D-luciferin significantly at 90% IC_{50} and 45% IC_{50} values, which indicated that these TCM components could slow down the outflow of D-luciferin from MCF-7/DOX^{Fluc} (Tables 1 and S1). Among these agents, the MDR reversing effect of Qu, which increased the AUC most obviously, was comparable to that of the positive control Vera (10 μg/mL)[23] (Figure 2C,D). These results suggested that Qu could be selected as an ideal MDR reversal agent.

Qu Significantly Suppressed the Efflux of D-Luciferin *In Vivo*, Consistent with the *In Vitro* Results. The MCF-7/DOX^{Fluc} tumor-bearing mice in the group receiving Qu (10 mg/kg)[24] and phosphate-buffered saline (PBS) treatment were injected with D-luciferin potassium salt (50 mg/kg, *i.p.*) at the time points of 7 and 14 days (Figure 3A) and then characterized by BLI (Figure 3B). BLI_{rel} of D-luciferin affected by Qu progressively increased and then decreased over time (Figure 3C,D). The parameters were calculated based on the non-compartmental model, and the mean residence time (MRT) of Qu (32.34 ± 0.72 min) was shorter than that of PBS (41.32 ± 0.63 min), while the AUC of Qu (167.73 ± 0.56) increased significantly compared to that of PBS (98.67 ± 0.52) on the 14th day (Figure 3E).

Pearson correlation analysis was applied to analyze the consistency via the AUC of the efflux curve of D-luciferin between *in vitro* and *in vivo* cases after Qu treatment. The results indicated that the AUC values *in vitro* and *in vivo* were positively correlated, with Pearson correlation coefficients of >0.7 (Pearson coefficient = 0.983) and associated P values of <0.05. Since the AUC of D-luciferin had a formidable correlation *in vitro* and *in vivo*, it could be a good indicator for screening MDR reversal agents in TCMs *in vitro*.

Qu Enhanced the Anti-Tumor Effect of DOX in MCF-7/DOX^{Fluc} Tumor-Bearing Mice. The above experiments demonstrated that Qu was chosen as an ideal reversal agent by this screening method with great consistent *in vitro* and *in vivo*. Then, we further validated the anti-tumor effect of the ideal reversal agent in combination with chemotherapeutic DOX. First of all, to determine the combination ratio of Qu to DOX, the combination index (CI) was calculated using an *in vitro* cellular assay. As a result, Qu increased the ability of DOX to suppress the growth of MCF-7/DOX^{Fluc} cells (Figure 4A). The findings demonstrated that Qu could synergistically strengthen inhibitory effect of DOX on cell proliferation. The ideal ratio of Qu to DOX was 2:1 (Figure 4B).

It was found that the Qu or DOX treatment slightly slowed the tumor growth in mice bearing MCF-7/DOX^{Fluc} compared to PBS, but DOX combined with Qu dramatically slowed tumor development (Figure 5A), including both the tumor volume (Figure 5B) and tumor mass (Figure 5C). Quantification of tumor fluorescence by BLI similarly showed that the combined group substantially inhibited tumor growth (Figure 5D−E). Moreover, the tumor tissues were nearly completely necrotic after the combined treatment of Qu and DOX, as demonstrated in the tumor sections by hematoxylin and eosin (H&E) staining (Figure 4F).

Qu Increased DOX Retention in the Tumor and Thus Maintained Its Effectiveness with Unobvious Toxicities by Low-Dosage Treatment. To detect whether Qu also delays the outflow of DOX in the tumor, the distribution of DOX within the tumor was assessed by HPLC at 0.5, 2, and 4 h following intravenous injection, and it was discovered that Qu helped free DOX accumulate more in the tumor site at all time points (Figures 6A and S3).

DOX has been well-known to cause serious side effects *in vivo*.[25] DOX alone (5 mg/kg) caused a significant decrease in body weight of MCF-7/DOX^{Fluc} tumor-bearing mice, and it seemed that Qu could not decrease the toxicities caused by DOX significantly (Figure 6B). Since Qu could increase DOX retention in the tumor, we tried to lower the dosage of DOX

https://doi.org/10.1021/acsomega.2c07096
ACS Omega 2023, 8, 4853−4861

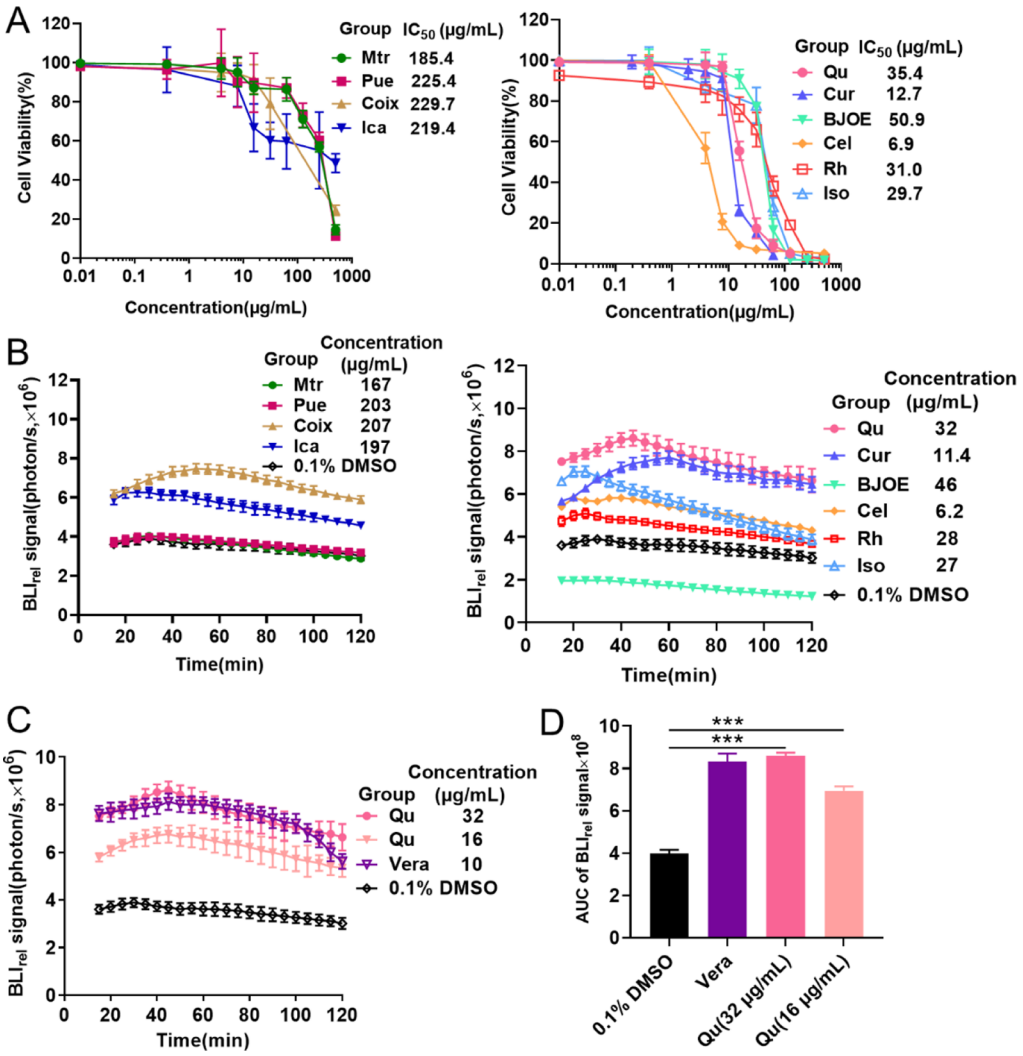

Figure 2. Qu was screened as a MDR reversal agent by fluorescence kinetics *in vitro*. (A) IC_{50} values of MCF-7/DOX^{Fluc} cells after the treatment with different TCMs for 48 h ($n = 6$). (B) BLI signal photon−time curve (90% IC_{50}) after 48 h of treatment with different TCMs. (C-D) Photon−time curve (C) of the BLI signal and AUC of the BLI_{rel} signal (D) after Qu (32 and 16 μg/mL) or Vera (10 μg/mL) treatment for 48 h ***$P < 0.001$.

Table 1. Effect of 90% IC_{50} of Different TCMs on Efflux Kinetics Parameters of D-Luciferin ($\bar{x} \pm s$, $n = 6$)[a]

	90% IC_{50} (μg/mL)	$t_{1/2}$ (min)	mean residence time (MRT) (min)	C_{max} (×106) (photon/s)	$AUC_{0-120min}$ (×10^8) photon/s × min
Pue	203	238.17 ± 50.42	353.83 ± 77.91	4.00 ± 0.33	4.12 ± 0.31
Mtr	167	164.63 ± 33.27	247.98 ± 46.52	4.04 ± 0.25	4.00 ± 0.16
Cur	11.4	227.07 ± 46.15	345.17 ± 84.34	7.71 ± 0.16***	7.72 ± 0.11***
Qu	32	232.73 ± 63.41	246.10 ± 62.38	8.61 ± 0.23***	8.60 ± 0.14***
Coix	207	169.54 ± 42.36	260.30 ± 58.64	7.47 ± 0.38**	7.62 ± 0.21**
BJOE	46	122.76 ± 47.35	187.23 ± 39.48	1.97 ± 0.15	1.87 ± 0.13
Ica	197	160.62 ± 30.27	243.65 ± 66.45	6.26 ± 0.18*	6.27 ± 0.26**
Cel	6.2	146.53 ± 37.22	225.58 ± 78.41	5.09 ± 0.27*	5.00 ± 0.43*
Rh	28	102.32 ± 53.04	158.31 ± 69.06	7.04 ± 0.34**	6.26 ± 0.39*
Iso	27	189.56 ± 67.82	282.55 ± 86.37	5.82 ± 0.16**	5.91 ± 0.17*
Vera		480.24 ± 81.58	211.43 ± 90.25	8.03 ± 0.29***	8.33 ± 0.37***
0.1% DMSO		191.94 ± 49.83	289.41 ± 70.53	3.88 ± 0.30	3.97 ± 0.18

[a]Note: compared with 0.1% DMSO, *$P < 0.05$,**$P < 0.01$, and ***$P < 0.001$.

to 2 mg/kg and determined whether DOX could keep its effectiveness and reduce its toxicity, caused by the high dose. It was found that DOX alone (2 mg/kg) caused just a little decrease of tumor cell proliferation compared with that of the PBS group, but DOX combined with Qu could dramatically delay tumor growth (Figure 6C). Also, when the DOX dosage was lowered to 2 mg/kg, it would not cause a significant body weight loss in both the DOX group and the combined group (Figure 6D). The histopathologic analysis also revealed no obvious toxicity by the H&E staining (Figure S4A). Additionally, biochemical indicators such as blood urea nitrogen, creatinine, and alanine amino transaminase showed no

https://doi.org/10.1021/acsomega.2c07096
ACS Omega 2023, 8, 4853−4861

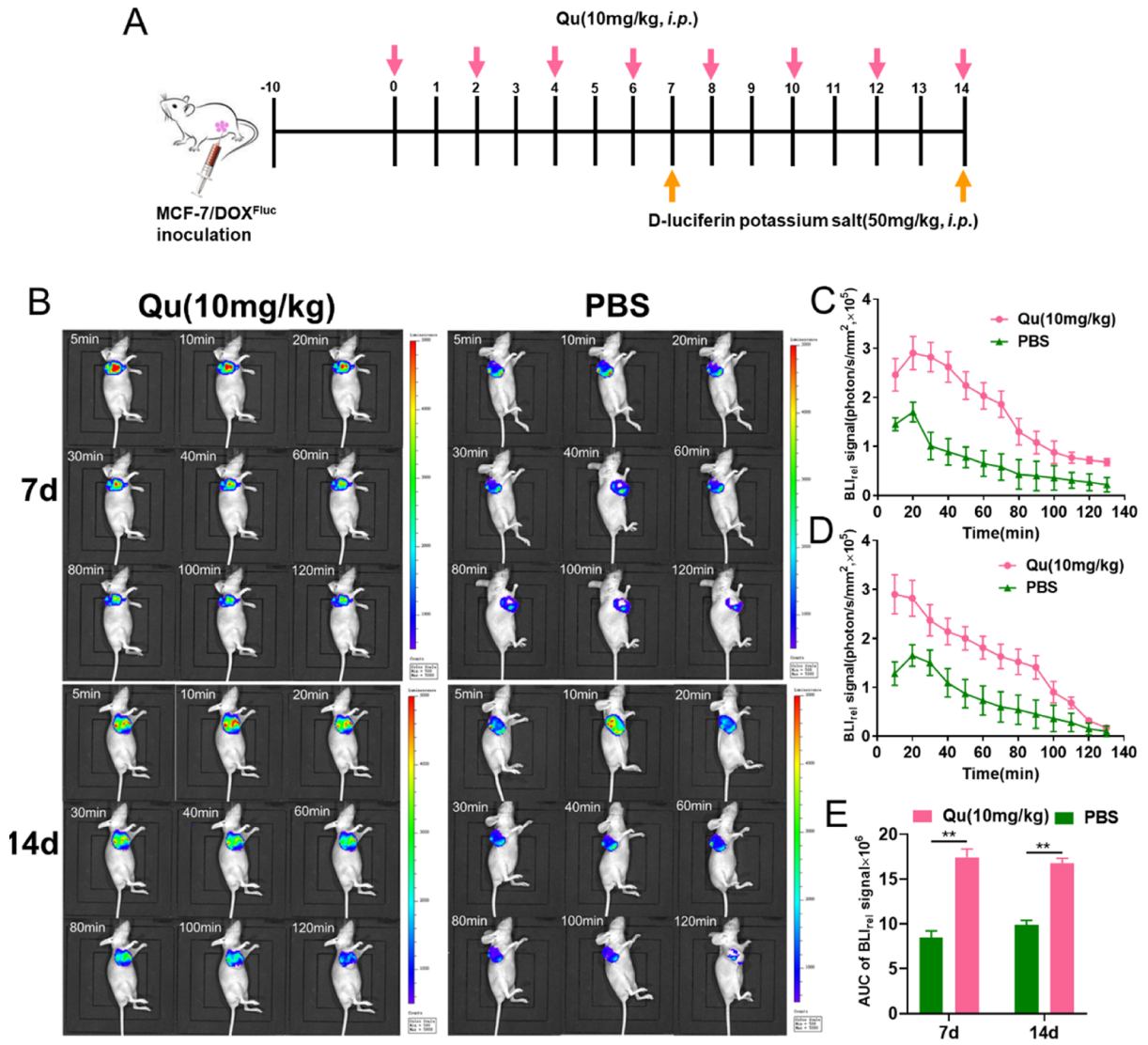

Figure 3. Qu enhanced D-luciferin retention in tumor. (A) Schematic illustration of the experimental design and treatment regimen in MCF-7/DOX^{Fluc} tumor-bearing mice. (B) Nude mice bearing MCF-7/DOX^{Fluc} tumor received BLI at diverse time points in 130 min after intraperitoneal injection of 50 mg/kg D-luciferin potassium salt. (C−D) Photon−time curve of the BLI$_{rel}$ signal in mice bearing MCF-7/DOX^{Fluc} tumor undergoing the Qu (10 mg/kg) treatment at day 7 (C) and day 14 (D). (E) AUC of the BLI$_{rel}$ signal after the Qu treatment. $^{**}P < 0.01$.

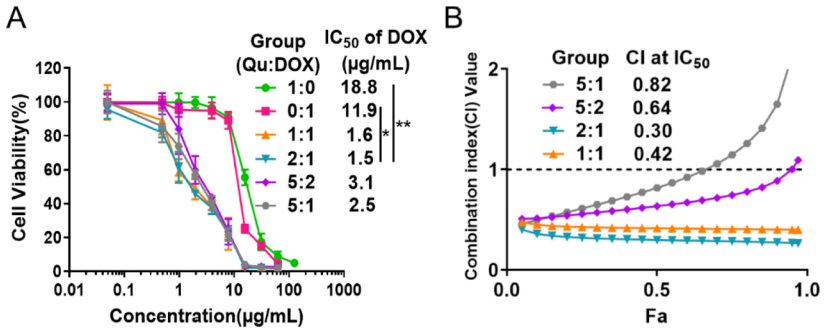

Figure 4. (A) MCF-7/DOX^{Fluc} cells treated with DOX and Qu at different ratios for 48 h ($n = 6$). (B) Corresponding CIs of MCF-7/DOX^{Fluc} cells undergoing DOX and Qu treatments for 48 h at different ratios. $^{*}P < 0.05$ and $^{**}P < 0.01$.

significant difference between all groups (Figure S4B). Above all, Qu could not decrease the toxicities of DOX directly, but it could increase DOX retention in the tumor, thus maintaining its effectiveness with unobvious toxicities by the low-dosage treatment.

CONCLUSIONS AND DISCUSSION

Drug resistance in cancer is a huge problem for patients all over the world.[26] Ample studies prove that cancer cells over-expressing ABC transporters are significantly associated with MDR, leading to treatment failure of chemotherapy.[27,28] Both

https://doi.org/10.1021/acsomega.2c07096
ACS Omega 2023, 8, 4853−4861

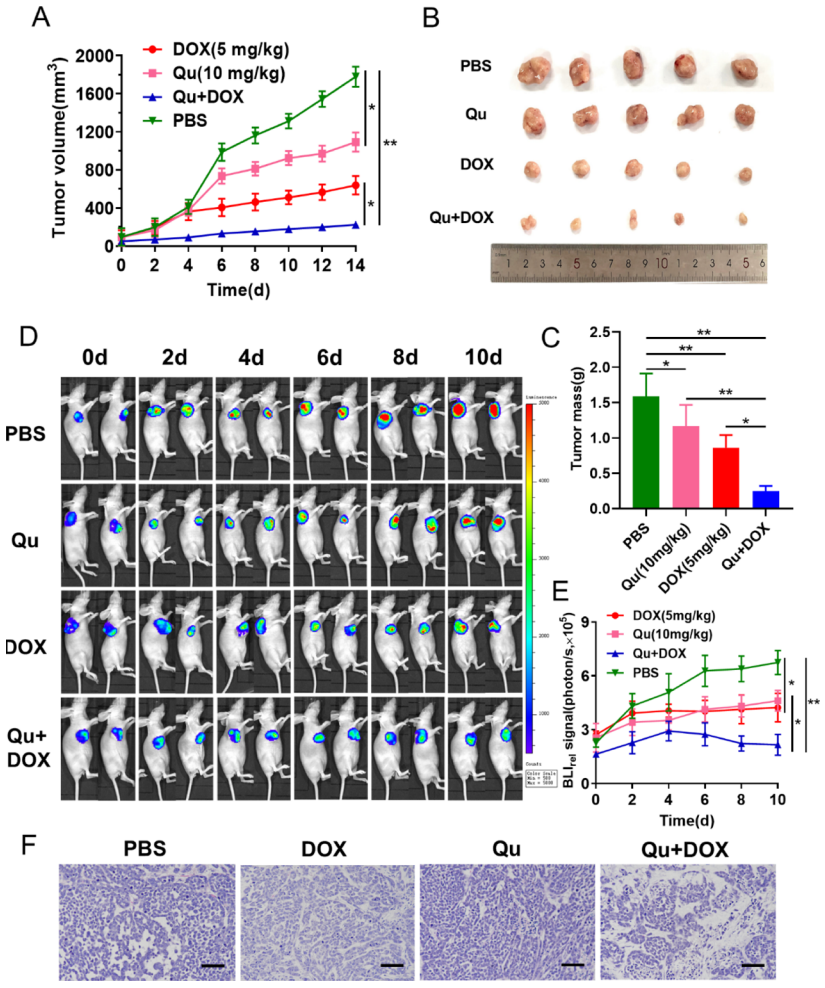

Figure 5. Qu increased the anti-tumor efficacy of DOX in the treatment of MCF-7/DOX^{Fluc} tumor. (A) Tumor volumes in MCF-7/DOX^{Fluc} tumor-bearing mice were treated with DOX (5 mg/kg, *i.v.*) and Qu (10 mg/kg, *i.p*). (B−C) Photographs (B) and tumor mass (C) of tumors excised from each treatment group. (D−E) In all the treatment groups, the BLI signal was recorded after the intravenous injection of 50 mg/kg D-luciferin potassium salt. (F) H&E staining was performed on the tumors of MCF-7/DOX^{Fluc} tumor-bearing nude mice after different treatments (Scale bars: 200 μm). $^{*}P < 0.05$ and $^{**}P < 0.01$.

clinical practice and pharmacological studies have found when combined with other first-line chemotherapy drugs, many active TCM ingredients are shown to be efficacious in reversing MDR and enhancing the efficacy of chemotherapeutic drugs.[29,30] Due to the wide variety of TCMs, it is of great importance to establish a method to screen MDR reversal agents from TCMs conveniently and simply.

The drugs screened out by many presently available *in vitro* screening methods may not necessarily be effective *in vivo* because the complexity of the *in vivo* tumor microenvironment. The method we established in this manuscript could maintain the *in vitro* and *in vivo* consistency of the MDR reversing effect since it could monitor the efflux function of ABC transporters located in tumor cells. Here, in order to investigate the MDR reversal effect of a series of TCM monomers or formulations *in vitro*,[31−40] D-luciferin was used as the probe of ABC transporter's efflux function by BLI. BLI is an imaging technique that is always sensitive, convenient, and reliable and can be used to monitor the feature of the cells tagged reporter gene just like luciferase.[41]

As a result, Qu was selected to be an ideal MDR reversal agent, which could effectively decrease the outflow of D-luciferin in MCF-7/DOX^{Fluc} cells. The correlation of efflux kinetics parameters indicated that Qu had a strong consistency in reversing MDR *in vitro* and *in vivo*, which was further confirmed by the anti-tumor efficacy of Qu combined with DOX on mice. Besides, we also measured the distribution of DOX in tumors when combined with Qu, and the result could certify the feasibility of the *in vitro screening* method. Interestingly, although Qu was unable to reduce the toxicity of DOX directly, it enabled its effectiveness at a lower dose and thus reduce its toxicities. In conclusion, this study provided a novel, efficient, and inexpensive method to screen MDR reversal agents in TCMs. An important potential advantage of our method is that it could be applied to screen not only monomers but also compounds of TCMs.

MATERIALS AND METHODS

Materials. DOX was obtained from Aladdin (Shanghai, China). Coix was obtained from Kanglaite (Zhejiang, China). *Brucea javanica* oil emulsion (BJOE) was obtained from Dalei Yunshang Pharmaceutical Co., Ltd (Shenyang, China). Puerarin (Pue), matrine (Mtr), Cur, Qu, Iso, Cel, Rh, and Ica were bought from Macklin (Shanghai, China). The purity of these ingredients was more than 98%. D-luciferin was procured from Science Kight Biology Science & Technology (Shanghai,

https://doi.org/10.1021/acsomega.2c07096
ACS Omega 2023, 8, 4853−4861

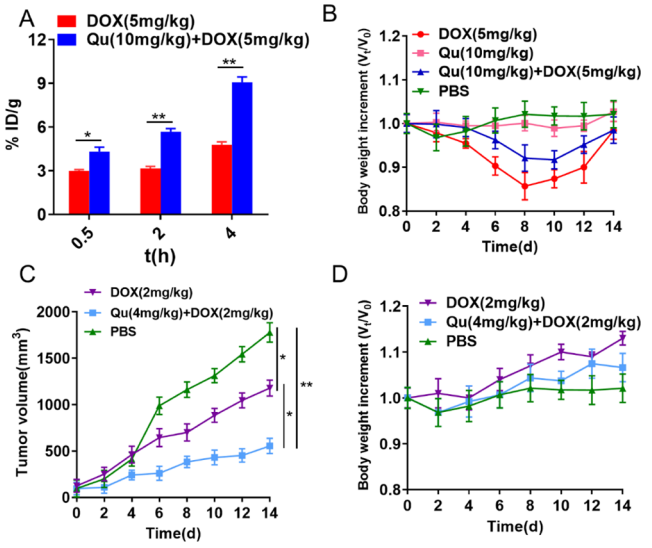

Figure 6. Qu enhanced the efficacy and mitigates the toxicity of DOX by increasing its retention in tumor. (A) Distribution of DOX in the tumor by DOX (5 mg/kg, *i.v.*) alone or combined with Qu (10 mg/kg, *i.p.*) treatment for 0.5, 2, and 4 h. (B) Body weight increment of mice after being treated with PBS, DOX (5 mg/kg), Qu (10 mg/kg), and DOX (5 mg/kg) and Qu (10 mg/kg). (C) Tumor volume and (D) body weight increment of mice due to DOX (2 mg/kg, *i.v.*) alone or combined with the Qu treatment (4 mg/kg, *i.p*). $^{*}P < 0.05$ and $^{**}P < 0.01$.

China). DMSO and MTT were procured from Sigma-Aldrich (St. Louis, MO, USA). RIPA and BCA kits were procured from Beyotime Biotechnology (Shanghai, China). Verapamil (Vera) was procured from Apexbio (Houston, USA). All chemicals for the experiment were of analytical reagent grade.

Cell Lines and Animals. The MCF-7/DOX cells were supplied by the West China Pharmacy School of Pharmacy, Sichuan University. The resistance index of MCF-7/DOX was 131.7.[42] In our previous study, an MCF-7/DOX^{Fluc} cell line stably expressing the firefly luciferase reporter gene was prepared by lentiviral infection.[43] BALB/c nude mice (4 weeks, female) were supplied from Slake Laboratory Animal Company (Shanghai, China) and housed in the Laboratory Animal Center at Zhejiang Chinese Medical University (Hangzhou, China). In order to perform the xenograft models, 6×10^7 of MCF-7/DOX^{Fluc} cells were inoculated subcutaneously into the right side of mice. Subcutaneous tumors developed to 80∼100 mm^3 after inoculation for 8−10 days. The procedures concerning animals were carried out in agreement with the protocol allowed by the Zhejiang Chinese Medical University Laboratory Animal Research Center with the approval number 10248.

IC_{50} of MDR Reversal Agents on MCF-7/DOX^{Fluc} Cells. MCF-7/DOX^{Fluc} cells were incubated with 8×10^4 cells/well in 100 μL of RMPI 1640 medium in 96-well plates. MTT was formulated to 5 mg/mL. Different concentrations of Pue, Mtr, Cur, Qu, Coix, BJOE, Rh, Cel, Ica, and Iso were incubated with the MCF-7/DOX^{Fluc} cells for 48 h, and then, 100 μL of the MTT solution was added and incubated for 4 h. Thereafter, the medium was carefully discarded, and 100 μL of DMSO was added. Before testing the absorbance at 490 nm on the microplate reader, the plate was gently shaken for 10 min. The cell proliferation and IC_{50} values were then calculated by using GraphPad Prism V6.01 software.

Efflux Kinetics of D-Luciferin from MCF-7/DOX^{Fluc} Cells *In Vitro*. MCF-7/DOX^{Fluc} cells were seeded on a 96-well flat-bottom black plates at 8×10^3 cells/well. In order to study the effect of different TCMs on the efflux function mediated by ABC transporters *in vitro*, BLI was used to quantitatively monitor the outflow of D-luciferin in real time from MCF-7/DOX^{Fluc} cells, which were treated by different TCM ingredients at the 90% or 45% IC_{50} value. Eight TCM monomer components (Pue, Mtr, Cur, Qu, Iso, Cel, Rh, and Ica) and two kinds of TCM formulations (Coix and BJOE) were chosen as MDR reversal agents, and MTT was used to measure the IC_{50} value of these agents on MCF-7/DOX^{Fluc}. The changes of all of the efflux curves with time were drawn.

Then, MCF-7/DOX^{Fluc} cells were treated with the ideal reversal agent for 48 h. Vera (a *P*-gp inhibitor, 10 μg/mL)[44] was applied alone as a positive control. Thereafter, D-luciferin (10 μg/mL) was added, and an *in vivo* imaging system (IVIS) (Xenon, USA) was used for kinetic imaging immediately. The excreted extracellular signals were caught every 5 min for 0−130 min to obtain the efflux kinetics of D-luciferin. The photon signal was standardized to the relative bioluminescence imaging (BLI_{rel}) by the total protein concentration to remove the disturbing effect. Kinetic parameters of intracellular D-luciferin were counted on the basis of the non-atrial model method.[45]

Efflux Kinetics of D-Luciferin in Mice Bearing MCF-7/DOX^{Fluc}. Qu (10 mg/kg) was administered every 2 days, and D-luciferin was injected on the 7th and 14th day, respectively. The mice were intraperitoneally injected with 50 mg/kg D-luciferin, and then, the BLI signal was quantitatively recorded in 130 min. The photon signal was standardized depending on the tumor volume and considered as BLI_{rel}. The non-compartmental model was used to calculate the AUC and MRT of D-luciferin.

Correlation Analysis *In Vivo* and *In Vitro*. The AUC of the outflowed D-luciferin by ABC transporters was adopted as the indicator of the efflux kinetics of D-luciferin after the treatment with the ideal reversal agent. Relationship of the efflux kinetics of D-luciferin *in vitro* and *in vivo* was analyzed by Pearson correlation analysis.

CI Studies cetween the Ideal Agent and DOX. The MTT assay was applied to evaluate the cytotoxicity and the MDR reversal effect of the ideal agent. Cells were seeded into 96-well plates at 8×10^3 cells/well for 24 h before drug treatment. Soon after, tumor cells were incubated and then were exposed to DOX and Qu at an appropriate ratio to measure the cell viability. The cell viability was calculated by using CompuSyn software to analyze the CI by the Chou and Talalay method.

Combined Anti-Tumor Efficacy of the Ideal Agent and DOX *In Vivo*. Nude mice bearing MCF-7/DOX^{Fluc} tumor were applied to assess the antitumor effect. Mice were randomly divided into four groups ($n = 6$) and, respectively, treated by PBS, DOX (5 mg/kg, *i.v*), Qu (10 mg/kg, *i.p*), and DOX (5 mg/kg, *i.v.*) combined with Qu (10 mg/kg, *i.p.*) every 2 days. Also, the body weight and the tumor volumes were recorded. The tumor volume (V) was calculated from the length (L) and width (W), in view of the following equation: $V = (1/2 \times L \times W^2)$. Every other day after the treatment, 100 μL of D-fluorescein potassium salt (50 mg/kg) was injected intraperitoneally, and the mice bearing MCF-7/DOX^{Fluc} tumor were imaged immediately via IVIS to document the fluorescence peak. BLI signals of MCF-7/DOX^{Fluc} were tested at Ex = 328 nm and Em = 533 nm. Then, hearts, livers, spleens, lungs, kidneys, and tumors were gathered to estimate the systemic toxicity by H&E staining.

https://doi.org/10.1021/acsomega.2c07096
ACS Omega 2023, 8, 4853−4861

Distribution of DOX in the Tumor. Mice were randomly grouped into two groups of treatments: DOX alone or combined with Qu. The mice were fasted 12 h before the experiment and freely drank water. The mice were executed at 0.5, 2, and 4 h after the treatment, respectively. The tumors were excised, rinsed, and dried. Tumor weights were recorded. Then, 0.5 mL (0.25 g/mL) of each tumor tissue homogenate was transferred to a glass centrifuge tube, and 2 mL of methanol−chloroform (1:4, v/v) was added to extract the sample. Then, the homogenate was shaken for 5 min and then centrifuged at 15,000 rpm for 5 min to collect the supernatant, which was then dried under nitrogen. The dried residue was reconstituted with 100 μL of methanol, and then, the concentration of DOX was analyzed by HPLC (Waters, USA). The Aglient ZORBAX Eclipse Plus C18 column (4.6 mm × 250 mm, 5 μm) was used to detect at 25 °C with a mobile phase of 0.1% H_3PO_4: acetonitrile: methanol = 25:25:3 (v/v/v) at a flow rate of 1 mL/min. The wavelength of 254 μm was used for the detection. DOX content in the tumor was detected by HPLC, and calibration curves were established by analyzing different concentrations of tumor samples. The calibration curves could be described by the following regression equation: Y = 676.96C + 1023.8. The calibration curves of DOX concentration exhibited good linearity (R^2 = 0.98) over a concentration range of 0.05−80 μg/mL.

Statistical Analysis. Data were expressed as the mean ± SD for a minimum of three experiments. The comparison between two groups was conducted by the unpaired t-test, and one-way ANOVA was used for multiple groups. A difference was deemed statistically significance if $P < 0.05$.

■ ASSOCIATED CONTENT

Supporting Information

The Supporting Information is available free of charge at https://pubs.acs.org/doi/10.1021/acsomega.2c07096.

The relationship between the fluorescence signal and D-luciferin concentration; the relationship between the fluorescence signal and cell number of MCF-7/DOX^{Fluc}; the specificity of DOX in the tumor by HPLC; BLI signal photon−time curve (45% IC_{50}) after 48 h of treatment with different TCMs; H&E staining of major organs of mice; and serum liver and kidney indexes of mice in each administration group (PDF)

■ AUTHOR INFORMATION

Corresponding Author

Yang Xiong − *College of Pharmaceutical Sciences and Academy of Chinese Medical Science, Zhejiang Chinese Medical University, Hangzhou, Zhejiang 311258, China;* orcid.org/0000-0002-9508-1987; Phone: +86-571-61768158; Email: xyxnb@126.com

Authors

Yue Zhao − *College of Pharmaceutical Sciences and Academy of Chinese Medical Science, Zhejiang Chinese Medical University, Hangzhou, Zhejiang 311258, China*

Chaoyuan Tang − *College of Pharmaceutical Sciences, Zhejiang Chinese Medical University, Hangzhou, Zhejiang 311258, China; Changxing People's Hospital of Zhejiang, Huzhou, Zhejiang 313100, China*

Jingyi Huang − *College of Pharmaceutical Sciences, Zhejiang Chinese Medical University, Hangzhou, Zhejiang 311258, China*

Hongyan Zhang − *College of Pharmaceutical Sciences, Zhejiang Chinese Medical University, Hangzhou, Zhejiang 311258, China*

Jingbin Shi − *College of Pharmaceutical Sciences, Zhejiang Chinese Medical University, Hangzhou, Zhejiang 311258, China*

Shujun Xu − *College of Pharmaceutical Sciences, Zhejiang Chinese Medical University, Hangzhou, Zhejiang 311258, China*

Lisha Ma − *College of Pharmaceutical Sciences, Zhejiang Chinese Medical University, Hangzhou, Zhejiang 311258, China*

Chun Peng − *School of Medical Technology and Information Engineering, Zhejiang Chinese Medical University, Hangzhou, Zhejiang 310053, China*

Qi Liu − *Department of Dermatology, Johns Hopkins University School of Medicine, Baltimore, Maryland 21231, United States*

Complete contact information is available at: https://pubs.acs.org/10.1021/acsomega.2c07096

Author Contributions

#Y.Z., C.-Y.T., and J.-Y.H. contributed equally to this work.

Notes

The authors declare no competing financial interest.

■ ACKNOWLEDGMENTS

This work was supported by the National Natural Science Foundation of Zhejiang Province (grant number LZ22H290001) and the Medical and Health Science and Technology Program of Zhejiang Province (grant number 2021KY813). We appreciate the great support from the Public Platform of Pharmaceutical Research Center, Academy of Chinese Medical Science, Zhejiang Chinese Medical University.

■ REFERENCES

(1) Siegel, R. L.; Miller, K. D.; Fuchs, H. E.; Jemal, A. Cancer statistics, 2022. *CA Cancer J Clin* **20222022**, *72*, 7−33.

(2) Singh, D.; Assaraf, Y. G.; Gacche, R. N. Long non-coding RNA mediated drug resistance in breast cancer. *Drug resist update* **2022**, *63*, 100851.

(3) Wei, G.; Wang, Y.; Yang, G.; Wang, Y.; Ju, R. Recent progress in nanomedicine for enhanced cancer chemotherapy. *Theranostics* **2021**, *11*, 6370−6392.

(4) Liu, S.; Khan, A. R.; Yang, X.; Dong, B.; Ji, J.; Zhai, G. The reversal of chemotherapy-induced multidrug resistance by nanomedicine for cancer therapy. *J Control Release* **2021**, *335*, 1−20.

(5) Stefan, S. M.; Wiese, M. Small-molecule inhibitors of multidrug resistance-associated protein 1 and related processes: A historic approach and recent advances. *Med. Res. Rev.* **2019**, *39*, 176−264.

(6) Li, X.; Song, Y.; Wang, L.; Kang, G.; Wang, P.; Yin, H.; Huang, H. A Potential Combination Therapy of Berberine Hydrochloride With Antibiotics Against Multidrug-Resistant Acinetobacter baumannii. *Front Cell Infect Microbiol* **2021**, *11*, 660431.

(7) Sui, X. B.; Xie, T. Combination of Chinese and Western Medicine to Prevent and Reverse Resistance of Cancer Cells to Anticancer Drugs. *Chin J Integr Med* **2020**, *26*, 251−255.

(8) Ma, X.; Hu, M.; Wang, H.; Li, J. Discovery of traditional Chinese medicine monomers and their synthetic intermediates, analogs or derivatives for battling P-gp-mediated multi-drug resistance. *Eur. J. Med. Chem.* **2018**, *159*, 381−392.

(9) Wei, J.; Liu, Z.; He, J.; Liu, Q.; Lu, Y.; He, S.; Yuan, B.; Zhang, J.; Ding, Y. Traditional Chinese medicine reverses cancer multidrug resistance and its mechanism. *Clin. Transl. Oncol.* **2022**, *24*, 471−482.
(10) Robey, R. W.; Pluchino, K. M.; Hall, M. D.; Fojo, A. T.; Bates, S. E.; Gottesman, M. M. Revisiting the role of ABC transporters in multidrug-resistant cancer. *Nat. Rev. Cancer* **2018**, *18*, 452−464.
(11) Wang, J. Q.; Yang, Y.; Cai, C. Y.; Teng, Q. X.; Cui, Q.; Lin, J.; Assaraf, Y. G.; Chen, Z. S. Multidrug resistance proteins (MRPs): Structure, function and the overcoming of cancer multidrug resistance. *Drug resist updat* **2021**, *54*, 100743.
(12) Li, W.; Zhang, H.; Assaraf, Y. G.; Zhao, K.; Xu, X.; Xie, J.; Yang, D. H.; Chen, Z. S. Overcoming ABC transporter-mediated multidrug resistance: Molecular mechanisms and novel therapeutic drug strategies. *Drug Resist Updat* **2016**, *27*, 14−29.
(13) Giddings, E. L.; Champagne, D. P.; Wu, M. H.; Laffin, J. M.; Thornton, T. M.; Valenca-Pereira, F.; Culp-Hill, R.; Fortner, K. A.; Romero, N.; East, J.; Cao, P.; Arias-Pulido, H.; Sidhu, K. S.; Silverstrim, B.; Kam, Y.; Kelley, S.; Pereira, M.; Bates, S. E.; Bunn, J. Y.; Fiering, S. N.; Matthews, D. E.; Robey, R. W.; Stich, D.; D'Alessandro, A.; Rincon, M. Mitochondrial ATP fuels ABC transporter-mediated drug efflux in cancer chemoresistance. *Nature communications* **2021**, *12*, 2804.
(14) Chen, Z.; Shi, T.; Zhang, L.; Zhu, P.; Deng, M.; Huang, C.; Hu, T.; Jiang, L.; Li, J. Mammalian drug efflux transporters of the ATP binding cassette (ABC) family in multidrug resistance: A review of the past decade. *Cancer Lett* **2016**, *370*, 153−164.
(15) Sampson, A.; Peterson, B. G.; Tan, K. W.; Iram, S. H. Doxorubicin as a fluorescent reporter identifies novel MRP1 (ABCC1) inhibitors missed by calcein-based high content screening of anticancer agents. *Biomed Pharmacother* **2019**, *118*, 109289.
(16) Wang, J.; Yang, D. H.; Yang, Y.; Wang, J. Q.; Cai, C. Y.; Lei, Z. N.; Teng, Q. X.; Wu, Z. X.; Zhao, L.; Chen, Z. S. Overexpression of ABCB1 Transporter Confers Resistance to mTOR Inhibitor WYE-354 in Cancer Cells. *Int. J. Mol. Sci.* **2020**, *21*, 1387.
(17) Zeng, Z.; Liao, S.; Zhou, H.; Liu, H.; Lin, J.; Huang, Y.; Zhou, C.; Xu, D. Novel Sigma-2 receptor ligand A011 overcomes MDR in adriamycin-resistant human breast cancer cells by modulating ABCB1 and ABCG2 transporter function. *Front Pharmacol* **2022**, *13*, 952980.
(18) Zhang, Z.; Ma, C.; Li, P.; Wu, M.; Ye, S.; Fu, L.; Xu, J. Reversal effect of FW-04-806, a macrolide dilactone compound, on multidrug resistance mediated by ABCB1 and ABCG2 in vitro and in vivo. *Cell Commun Signal* **2019**, *17*, 110.
(19) Miheecheva, N.; Postovalova, E.; Lyu, Y.; Ramachandran, A.; Bagaev, A.; Svekolkin, V.; Galkin, I.; Zyrin, V.; Maximov, V.; Lozinsky, Y.; Isaev, S.; Ovcharov, P.; Shamsutdinova, D.; Cheng, E. H.; Nomie, K.; Brown, J. H.; Tsiper, M.; Ataullakhanov, R.; Fowler, N.; Hsieh, J. J. Multiregional single-cell proteogenomic analysis of ccRCC reveals cytokine drivers of intratumor spatial heterogeneity. *Cell Rep* **2022**, *40*, 111180.
(20) Mirzaei, S.; Gholami, M. H.; Hashemi, F.; Zabolian, A.; Farahani, M. V.; Hushmandi, K.; Zarrabi, A.; Goldman, A.; Ashrafizadeh, M.; Orive, G. Advances in understanding the role of P-gp in doxorubicin resistance: Molecular pathways, therapeutic strategies, and prospects. *Drug Discov Today* **2022**, *27*, 436−455.
(21) Zhang, Y.; Pullambhatla, M.; Laterra, J.; Pomper, M. G. Influence of bioluminescence imaging dynamics by D-luciferin uptake and efflux mechanisms. *Mol Imaging* **2012**, *11*, 499−506.
(22) Qian, Y.; Xiong, Y.; Feng, D.; Wu, Y.; Zhang, X.; Chen, L.; Gu, M. Coix Seed Extract Enhances the Anti-Pancreatic Cancer Efficacy of Gemcitabine through Regulating ABCB1- and ABCG2-Mediated Drug Efflux: A Bioluminescent Pharmacokinetic and Pharmacodynamic Study. *Int. J. Mol. Sci.* **2019**, *20*, 5250.
(23) Maimaitijiang, A.; Wang, B.; Yang, H.; Tang, D.; Liu, Y.; Aisa, H. A. Discovery of a novel highly potent and low-toxic jatrophane derivative enhancing the P-glycoprotein-mediated doxorubicin sensitivity of MCF-7/ADR cells. *Eur. J. Med. Chem.* **2022**, *244*, 114822.
(24) Chuang, C. H.; Lin, Y. C.; Yang, J.; Chan, S. T.; Yeh, S. L. Quercetin supplementation attenuates cisplatin induced myelosuppression in mice through regulation of hematopoietic growth factors and hematopoietic inhibitory factors. *J. Nutr. Biochem.* **2022**, *110*, 109149.
(25) Wang, Y.; Yi, Y.; Yao, J.; Wan, H.; Yu, M.; Ge, L.; Zeng, X.; Wu, M.; Mei, L. Isoginkgetin synergizes with doxorubicin for robust co-delivery to induce autophagic cell death in hepatocellular carcinoma *Acta biomaterialia*; Advance online publication, 2022, Vol. *22*, pp S174200597−S174270619.
(26) Rezayatmand, H.; Razmkhah, M.; Razeghian-Jahromi, I. Drug resistance in cancer therapy: the Pandora's Box of cancer stem cells. *Stem Cell Res Ther* **2022**, *13*, 181.
(27) Yao, M.; Ma, X.; Zhang, X.; Shi, L.; Liu, T.; Liang, X.; Zhao, H.; Li, X.; Li, L.; Gao, H.; Jia, B.; Wang, F. Lectin-Mediated pH-Sensitive Doxorubicin Prodrug for Pre-Targeted Chemotherapy of Colorectal Cancer with Enhanced Efficacy and Reduced Side Effects. *Theranostics* **2019**, *9*, 747−760.
(28) Wang, M.; Chen, W.; Chen, J.; Yuan, S.; Hu, J.; Han, B.; Huang, Y.; Zhou, W. Abnormal saccharides affecting cancer multi-drug resistance (MDR) and the reversal strategies. *Eur. J. Med. Chem.* **2021**, *220*, 113487.
(29) Gao, Y.; Chen, S.; Sun, J.; Su, S.; Yang, D.; Xiang, L.; Meng, X. Traditional Chinese medicine may be further explored as candidate drugs for pancreatic cancer: A review. *Phytother Res* **2021**, *35*, 603−628.
(30) Su, X. L.; Wang, J. W.; Che, H.; Wang, C. F.; Jiang, H.; Lei, X.; Zhao, W.; Kuang, H. X.; Wang, Q. H. Clinical application and mechanism of traditional Chinese medicine in treatment of lung cancer. *Chin Med J* **2020**, *133*, 2987−2997.
(31) Liu, Q.; Wang, C.; Meng, Q.; Wu, J.; Sun, H.; Sun, P.; Ma, X.; Huo, X.; Liu, K. Puerarin sensitized K562 / ADR cells by inhibiting NF-κB pathway and inducing autophagy. *Phytother Res* **2021**, *35*, 1658−1668.
(32) Ashrafizadeh, M.; Zarrabi, A.; Hashemi, F.; Moghadam, E. R.; Hashemi, F.; Entezari, M.; Hushmandi, K.; Mohammadinejad, R.; Najafi, M. Curcumin in cancer therapy: A novel adjunct for combination chemotherapy with paclitaxel and alleviation of its adverse effects. *Life Sci.* **2020**, *256*, 117984.
(33) Yang, C.; Hou, A.; Yu, C.; Dai, L.; Wang, W.; Zhang, K.; Shao, H.; Ma, J.; Xu, W. Kanglaite reverses multidrug resistance of HCC by inducing apoptosis and cell cycle arrest via PI3K/AKT pathway. *Onco Targets Ther* **2018**, *11*, 983−996.
(34) Qiu, Z. H.; Zhang, W. W.; Zhang, H. H.; Jiao, G. H. Brucea javanica oil emulsion improves the effect of radiotherapy on esophageal cancer cells by inhibiting cyclin D1-CDK4/6 axis. *World J Gastroenterol* **2019**, *25*, 2463−2472.
(35) Zhou, B. G.; Wei, C. S.; Zhang, S.; Zhang, Z.; Gao, H. M. Matrine reversed multidrug resistance of breast cancer MCF-7/ADR cells through PI3K/AKT signaling pathway. *J. Cell. Biochem.* **2018**, *119*, 3885−3891.
(36) Lu, X.; Yang, F.; Chen, D.; Zhao, Q.; Chen, D.; Ping, H.; Xing, N. Quercetin reverses docetaxel resistance in prostate cancer via androgen receptor and PI3K/Akt signaling pathways. *Int J Biol Sci* **2020**, *16*, 1121−1134.
(37) Hu, F. W.; Yu, C. C.; Hsieh, P. L.; Liao, Y. W.; Lu, M. Y.; Chu, P. M. Targeting oral cancer stemness and chemoresistance by isoliquiritigenin-mediated GRP78 regulation. *Oncotarget* **2017**, *8*, 93912−93923.
(38) Lin, F. Z.; Wang, S. C.; Hsi, Y. T.; Lo, Y. S.; Lin, C. C.; Chuang, Y. C.; Lin, S. H.; Hsieh, M. J.; Chen, M. K. Celastrol induces vincristine multidrug resistance oral cancer cell apoptosis by targeting JNK1/2 signaling pathway. *Phytomedicine* **2019**, *54*, 1−8.
(39) Teng, Y. N.; Kao, M. C.; Huang, S. Y.; Wu, T. S.; Lee, T. E.; Kuo, C. Y.; Hung, C. C. Novel application of rhein and its prodrug diacerein for reversing cancer-related multidrug resistance through the dual inhibition of P-glycoprotein efflux and STAT3-mediated P-glycoprotein expression. *Biomed Pharmacother* **2022**, *150*, 112995.
(40) Jiang, S.; Chang, H.; Deng, S.; Fan, D. Icariin enhances the chemosensitivity of cisplatinresistant ovarian cancer cells by suppressing autophagy via activation of the AKT/mTOR/ATG5 pathway. *Int J Oncol* **2019**, *54*, 1933−1942.

https://doi.org/10.1021/acsomega.2c07096
ACS Omega 2023, 8, 4853−4861

(41) Zambito, G.; Chawda, C.; Mezzanotte, L. Emerging tools for bioluminescence imaging. *Curr. Opin. Chem. Biol.* **2021**, *63*, 86−94.
(42) Qian, K.; Tang, C. Y.; Chen, L. Y.; Zheng, S.; Zhao, Y.; Ma, L. S.; Xu, L.; Fan, L. H.; Yu, J. D.; Tan, H. S.; Sun, Y. L.; Shen, L. L.; Lu, Y.; Liu, Q.; Liu, Y.; Xiong, Y. Berberine Reverses Breast Cancer Multidrug Resistance Based on Fluorescence Pharmacokinetics In Vitro and In Vivo. *ACS omega* **2021**, *6*, 10645−10654.
(43) Zhu, L. X.; Tang, C. Y.; Yu, J. D.; Chen, Z.; Xiong, Y. Impact of Coix seed oil on fluorescence excretion pharmacokinetics and protein expression in doxorubicin-resistant cells MCF-7/DOX. *Acta Pharmaceutica Sinica* **2018**, *53*, 84−89.
(44) Guo, Y.; He, W.; Yang, S.; Zhao, D.; Li, Z.; Luan, Y. Co-delivery of docetaxel and verapamil by reduction-sensitive PEG-PLGA-SS-DTX conjugate micelles to reverse the multi-drug resistance of breast cancer. *Colloids Surf B Biointerfaces* **2017**, *151*, 119−127.
(45) Tang, C. Y.; Zhu, L. X.; Yu, J. D.; Chen, Z.; Gu, M. C.; Mu, C. F.; Liu, Q.; Xiong, Y. Effect of β-elemene on the kinetics of intracellular transport of d-luciferin potassium salt (ABC substrate) in doxorubicin-resistant breast cancer cells and the associated molecular mechanism. *Eur. J. Pharm. Sci.* **2018**, *120*, 20−29.

https://doi.org/10.1021/acsomega.2c07096
ACS Omega 2023, 8, 4853−4861